

Frequency-tunable micromechanical oscillator

M. Zalalutdinov,^{a)} B. Ilic, D. Czaplewski, A. Zehnder, H. G. Craighead, and J. M. Parpia
Cornell Center for Materials Research, Ithaca, New York 14853-2501

(Received 8 June 2000; accepted for publication 18 September 2000)

An experimental method, employing a scanning tunneling microscope (STM) as an actuator and a scanning electron microscope (SEM) as a motion detector, was developed to study microelectromechanical systems (MEMS) and has been applied to study microfabricated cantilever beams. Vibrations actuated by an ac voltage applied to the piezodrive are transferred to the sample by the STM tip, which also provides a constraint at the drive location, altering the fundamental mode of the oscillation. A continuous change in the resonant frequency of the cantilever is achieved by varying the position of the STM tip. In contrast to the few percent tunability previously demonstrated for MEMS oscillators, we have varied the cantilever frequency over a 300% range.

© 2000 American Institute of Physics. [S0003-6951(00)03146-6]

Micromechanical oscillators are the basic component of numerous devices, such as scanning probe microscopes,^{1,2} ultrasensitive magnetometers,^{3,4} electromechanical filters,^{5,6} and mass sensors.⁷ A fixed resonant frequency limits the applicability of microelectromechanical systems (MEMS). For example, integrated tunable high Q filters could significantly reduce size and power consumption of telecommunication devices.⁵ A broadband variable frequency micromechanical oscillator could form the basis of a micromechanical spectrum analyzer. Magnetic resonance force microscopy (MRFM)^{2,8} could also greatly benefit from development of a tunable cantilever detector.

These applications motivate efforts to achieve a broadband tunable micromechanical oscillator. Recently, a few percent tuning of the resonant frequency of MEMS devices was realized by applying a dc voltage between the moving structure and the fixed base to modify the effective spring constant.^{6,9} Stowe *et al.*¹⁰ used the van der Waals force in proximity of a surface to change the resonant frequency of an ultrathin cantilever (spring constant, $\kappa \sim 10^{-6}$ N/m) by a factor of three. However, the low spring constant precludes the operation of the device at high-frequencies where tunable resonators are most desirable.

In this letter, we demonstrate that the resonant frequency can be altered by 300% by applying to the mechanical oscillator a local driving force and constraint. Fine tuning can be achieved by moving the constraint location. We believe this concept can be successfully applied to very small and high-frequency MEMS oscillators.

The cantilevers were fabricated from low-stress silicon nitride. Prior to loading into the scanning tunneling microscope (STM) chamber the cantilever surface was coated with a 15 nm Au-Pd alloy to provide good tunneling conditions. Data obtained with $225 \times 20 \times 0.6 \mu\text{m}$ and $200 \times 20 \times 0.6 \mu\text{m}$ cantilevers is presented in this letter.

Our experimental setup to excite and detect cantilever oscillations is sited in an ultrahigh vacuum (UHV) version of a JEOL 4500XT STM, combined with a scanning electron microscope (SEM). The tungsten tip of the STM engaged at

the cantilever surface was used as a point-like actuator, via a small ac voltage applied to the z piezoelectrode to drive the STM tip with <0.1 nm amplitude in the direction perpendicular to the surface.

The motion is detected by scanning the SEM electron beam across the edge of the cantilever and analyzing the yield of the secondary electrons (video signal). The incident electron beam is tilted at 45° to the cantilever surface, so if the electron beam crosses the edge while the cantilever is oscillating out-of-plane, the video signal is modulated at the drive frequency with an amplitude corresponding to the difference in the intensity of the secondary electrons emitted from the cantilever surface or base material. The electron beam is scanned linearly (8 s for a single scan, at least ten scans are used for averaging) over a distance greater than the motion of the cantilever edge. Thus the ac component is observed on the video signal only during the portion of the scan when the e -beam intersects the cantilever edge. During the e -beam scan the spectrum analyzer repeatedly sweeps the STM drive frequency through the resonance in 0.4–0.8 s and accumulates the spectrum of the video signal. The position of the peak in the resulting spectrum provides the resonant frequency of the cantilever oscillations. The height of the accumulated resonance peak should be roughly proportional to the fraction of the time of the e -beam scan, during which the ac component is present on the video signal, i.e., to the amplitude of the mechanical motion of the cantilever. It is possible to map the deflection of various MEMS structures by focusing the electron beam at a series of points along the edge of the moving object. This method can be considered as complementary to the laser Doppler vibrometry technique¹¹ and is indispensable for sub- μm -size structures.

Figures 1(a) and 1(b) show the STM tip engaged at different locations along the cantilever. Figure 1(c) shows measured frequency spectra of the video signal. Spectrum (a) was obtained with the STM engaged at the “fixed” end of the cantilever [Fig. 1(a)]. The tip acts as a conventional piezodrive and excites oscillations with the free cantilever eigenfrequency ($f_0 = 9.69$ kHz). Spectrum (b) for the tip positioned in Fig. 1(b) (the STM tip is $45 \mu\text{m}$ from the cantilever base), shows a sharp resonance shifted to f^*

^{a)}Electronic mail: maxim@ccmr.cornell.edu

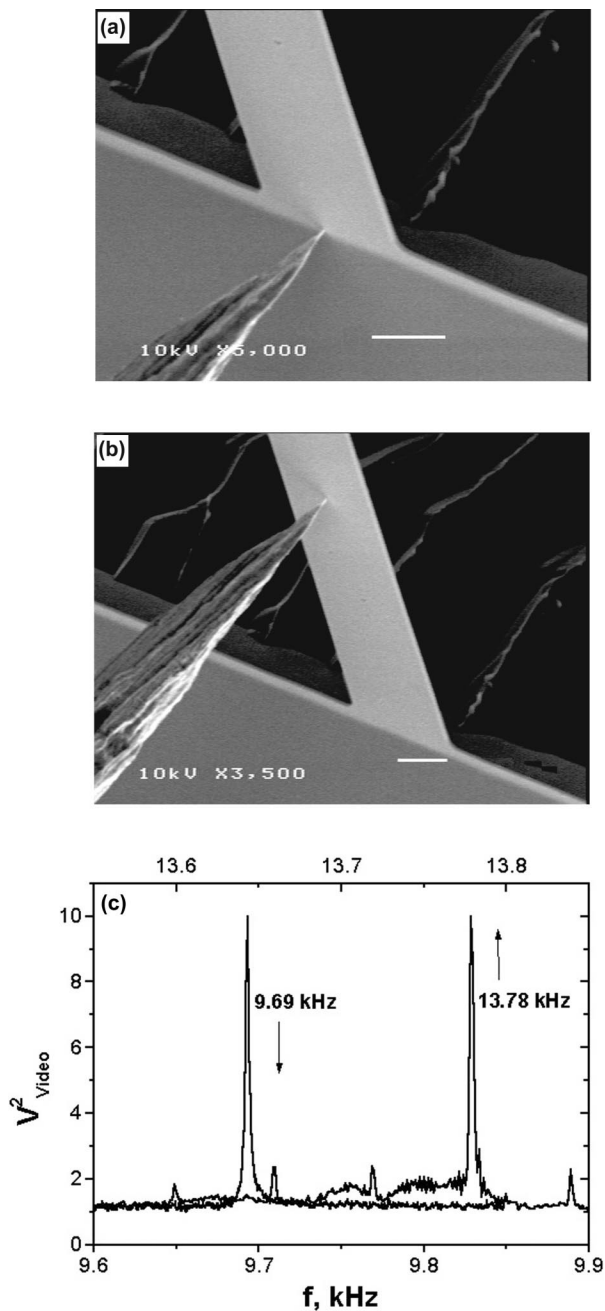


FIG. 1. Scanning electron micrographs (scale bar corresponds to $10\ \mu\text{m}$) of the silicon nitride cantilever with the STM tip engaged at the base (a) and $45\ \mu\text{m}$ away from the base of the cantilever (b). Plot (c) shows the corresponding resonant peaks acquired from the intensity of the secondary electrons (video signal).

$=13.78\ \text{kHz}$ and illustrates the concept of the position-dependent eigenfrequency of the cantilever.

Although the two resonance peaks in Fig. 1(c) have the same quality factor ($Q \sim 5000$), at many locations along the cantilever the width of the shifted resonance peak increases. We attribute the degradation of Q to the local variation of the surface contamination layer that acts as a damped spring between the STM tip and the cantilever. Research to understand the role of surface conditions on the cantilever Q is in progress.

Figure 2 shows the shift of the resonant frequency as a function of the STM tip position. P_{NORM} is the oscillation period normalized by the period of the free cantilever and

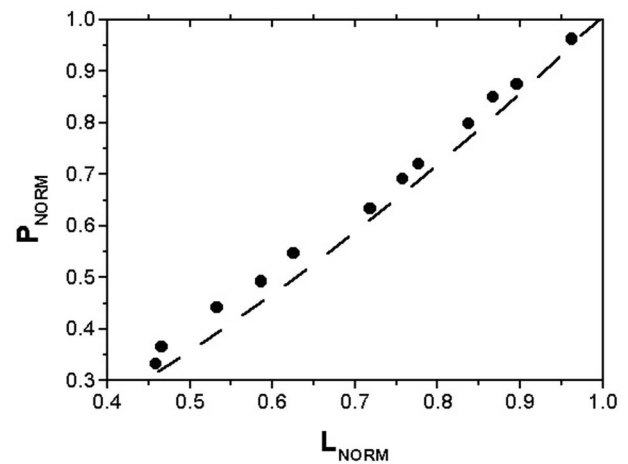


FIG. 2. Experimental data points and result of the calculations (dashed line) for the period of oscillations as a function of the STM tip position. The period P_{NORM} and active length L_{NORM} are normalized by the period of the free cantilever and the full length of the cantilever correspondingly.

L_{NORM} is the distance from the STM tip to the free end (active length) divided by the cantilever length. A continuously variable threefold increase of the resonant frequency without significant decrease of the amplitude of the cantilever vibration was detected as the STM was displaced toward the middle of the cantilever. Beyond the midpoint we found it difficult to excite and detect oscillations.

We attribute the observed frequency shift to a modification of the modes of the oscillator. At the point where the STM tip is engaged, the amplitude of the cantilever motion is restricted to less than $0.1\ \text{nm}$, in effect imposing an additional node that changes the boundary conditions and shifts the eigenfrequency. The beam deflection, $u(x, t)$ is governed by the equation of motion¹²

$$EI \frac{d^4 u}{dx^4} + \rho A \frac{d^2 u}{dt^2} = 0, \quad (1)$$

where E is the flexural modulus, I the moment of inertia, ρ

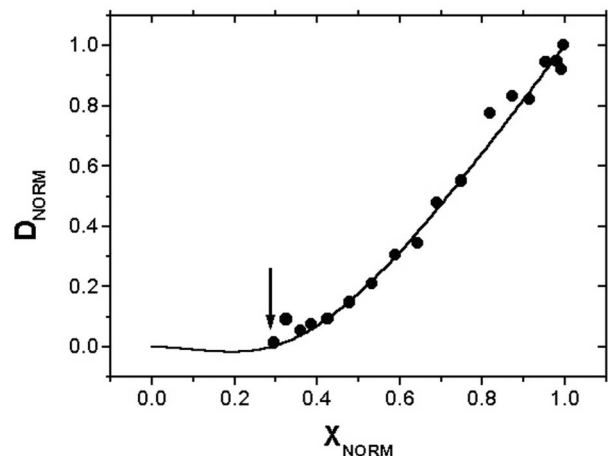


FIG. 3. Deflection curve, D_{NORM} normalized to the signal amplitude from the free end of the cantilever for the $200\ \mu\text{m}$ cantilever with the STM tip engaged $51\ \mu\text{m}$ from the base (tip location is indicated by the arrow). The solid line shows the calculated deflection, and experimental points represent the normalized height of the resonance peak on the spectrum of the video signal.

the density, and A the cross sectional area. Assuming a steady state response $u(x,t) = V(x)e^{i\omega t}$, yields an equation for $V(x)$:

$$\frac{d^4 V}{dx^4} - s^4 V = 0, \quad (2)$$

where

$$s^4 = \frac{\rho A}{EI} \omega^2.$$

For a cantilever of length L and a node located at ηL from the base of the cantilever ($0 \leq \eta \leq 1$), $V_1(x)$ describes the deflection for $x \leq \eta L$, while function $V_2(x)$ describes the deflection for $x \geq \eta L$. The full set of eight boundary conditions is:

$$\begin{aligned} V_1(0) = V_1'(0) = 0 & \quad \text{zero displacement and slope} \\ & \quad \text{at the fixed end} \\ V_1(\eta L) = V_2(\eta L) = 0 & \quad \text{zero displacement at the STM} \\ & \quad \text{tip (node)} \\ V_1'(\eta L) = V_2'(\eta L) & \quad \text{matching the slope at node} \\ V_1''(\eta L) = V_2''(\eta L) & \quad \text{matching the curvature or bending} \\ & \quad \text{moment at node} \\ V_2''(L) = 0 & \quad \text{zero moment at the free end} \\ V_2'''(L) = 0 & \quad \text{zero shear force at the free end.} \end{aligned}$$

The general solutions of Eq. (2) are

$$V_1(x) = A_1 \cos(sx) + B_1 \sin(sx) + C_1 \cosh(sx) + D_1 \sinh(sx), \quad (3)$$

$$V_2(x) = A_2 \cos[s(x - \eta L)] + B_2 \sin[s(x - \eta L)] + C_2 \cosh[s(x - \eta L)] + D_2 \sinh[s(x - \eta L)]. \quad (4)$$

Substitution of Eqs. (3) and (4) into the boundary conditions leads to a matrix equation for the coefficients $A_1, B_1, -D_2$. Solving the resulting nonlinear eigenvalue problem yields the period versus η , the position of the node. The dashed line in Fig. 2 shows the calculated result, which for $L_{\text{NORM}} = 1 - \eta > 0.45$ replicates the almost linear dependence of the period as a function of the normalized cantilever length. The calculations do not involve any fitting parameters and the agreement with the data is excellent.

Further comparison with the theoretical model was accomplished by acquiring the deflection curve at a fixed STM tip location, $51 \mu\text{m}$ from the base of the $200 \mu\text{m}$ cantilever. Spectra were acquired by shifting the focus of the electron beam to different points, x , along the cantilever. We plot the

normalized displacement, D_{NORM} against the position, $X_{\text{NORM}} = x/L$, of the electron beam. The amplitude of the cantilever vibrations at its free end is large enough so that it appears blurred on the SEM and can be used to provide an order of magnitude (200 nm) for the absolute value of the tip deflection shown in Fig. 3. The solid line in Fig. 3 shows the excellent agreement of the calculated deflection curve with the experimental data.

The theoretical model can provide guidance for the general case when a well-localized boundary condition (not necessarily a node) constrains the mechanical oscillator, providing a tuning mechanism. Our current implementation involving the STM tip is an illustration of this concept. The resonant frequency $f_0 \sim 10^4$ Hz was dictated by the bandwidth of the high-voltage amplifier for the STM piezodrive. Applicability of the SEM detection method is limited by the video amplifier bandwidth ($f \sim 10^6$ Hz). The basic principle of the local constraint could be scaled down to dimensions comparable with the STM tip radius (1–100 nm). We believe that tunable micromechanical oscillators will provide the basis for the realization of solutions for diverse applications.

In conclusion, we have developed a new method to drive and detect the motion of micromechanical oscillators, employing a STM and a SEM combination. The concept of a local drive force and constraint allows the cantilever resonance to be tuned over a 300% frequency range.

This work was supported by the Cornell Center for Materials Research (CCMR), supported by the NSF under Contract No. DMR-9632275. Fabrication was carried out at the Cornell Nanofabrication Facility, a member of the National Nanofabrication Users Network.

¹D. Sarid, *Scanning Force Microscopy with Applications to Electric, Magnetic and Atomic Forces* (Oxford University Press, New York, 1994).

²J. A. Sidles, J. L. Garbini, K. J. Bruland, D. Rugar, O. Zuger, S. Hoen, and C. S. Yannoni, *Rev. Mod. Phys.* **67**, 249 (1995).

³M. J. Naughton, J. P. Ulmet, A. Narjis, S. Askenazy, M. V. Cnabarala, and A. P. Hope, *Rev. Sci. Instrum.* **68**, 4061 (1997).

⁴C. Rossel, M. Willemin, A. Gasser, H. Bothuizen, G. I. Meijer, and H. Keller, *Rev. Sci. Instrum.* **69**, 3199 (1998).

⁵C. T.-C. Nguyen *Proc. SPIE* (to be published).

⁶C. T.-C. Nguyen, A.-C. Wong, and H. Ding, *Dig. Tech. Pap.-IEEE Int. Solid-State Circuits Conf.* **448**, 78 (1999).

⁷B. Ilic, D. Czaplewski, H. G. Craighead, P. Neuzil, C. Campagnolo, and C. Batt, *Appl. Phys. Lett.* **77**, 450 (2000).

⁸D. Rugar, C. S. Yannoni, and J. A. Sidles, *Nature (London)* **360**, 563 (1992).

⁹S. Evoy, D. W. Carr, L. Sekaric, A. Olkhovets, J. M. Parpia, and H. G. Craighead, *J. Appl. Phys.* **86**, 6072 (1999).

¹⁰T. D. Stowe, K. Yasumura, T. W. Kenny, D. Botkin, K. Wago, and D. Rugar, *Appl. Phys. Lett.* **71**, 288 (1997).

¹¹J. F. Vignola, S. F. Morse, X. Liu, L. Sekaric, B. H. Houston, and D. M. Photiadis, *Proc. SPIE* **4072** (2000).

¹²S. Timoshenko, D. H. Young, and W. Weaver, *Vibration Problems in Engineering* (Wiley, New York, 1974).